Research Article

Optimization of ANFIS controllers using improved ant colony to control an UAV trajectory tracking task

Boumediene Selma[1] · **Samira Chouraqui**[1] · **Hassane Abouaïssa**[2]

Received: 30 March 2019 / Accepted: 12 February 2020 / Published online: 10 April 2020

Abstract
Development of unmanned aerial vehicles (UAVs) has become the most important research areas in the field of autonomous aeronautical control. This paper proposes a robust and intelligent controller based on adaptive-network-based fuzzy inference system (ANFIS) and improved ant colony optimization (IACO) to govern the behavior of a three degree of freedom quadrotor UAV. The quadrotor was chosen due to its simple mechanical structure; nevertheless, these types of aircraft are highly nonlinear. Intelligent control such as fuzzy logic is a suitable choice for controlling nonlinear systems. The ANFIS controller is used to reproduce the desired trajectory of the quadrotor in 2D Vertical plane and the IACO algorithm aims is to facilitate convergence to the ANFIS's optimal parameters in order to reduce learning errors and improve the quality of the controller. To evaluate the performance of the proposed IACO tuned ANFIS controller, a comparison between the proposed ANFIS-IACO controller and other controller's performance such us ANFIS only and proportional–integral–derivative controllers is illustrated using the same system. As expected, the hybrid ANFIS-IACO controller gives very satisfactory results than the others methods already developed in the same study.

Keywords Unmanned aerial vehicle (UAV) · Intelligent control · Adaptive neuro-fuzzy inference system (ANFIS) · Improved ant colony optimization (IACO)

1 Introduction

The unmanned aerial vehicles (UAVs) technology has continuously been evolving with exceptional growth over the last years [1], leading to the emergence of a large number of services offered and potential applications. Drones are not meant to only serve with military purposes [2], but have also become widely used in civilian and industrial domain such us logistics and transportation [3–5], photography and filmmaking [6], safety and security [7], mapping [8], agriculture [9, 10], monitoring [11–14], surveillance [15–17], architecture [18–20] and others applications. They were originally used for missions tedious or too dangerous for humans and all this due to their ease of deployment, low maintenance cost [21], high mobility and hovering capability [22]. In general, UAVs are preferred for their ability to stabilize at a particular position and altitude [23], to fly at various speeds [24–26], to hover in a stationary position over a target [22, 27], and to perform all these maneuvers in close proximity to obstacles [28, 29].

The selection of the optimal controller parameters is a very important issue for every command and control problems in order to reduce learning errors and improve the quality of the controller [30, 31]. Engineers face daily with increasingly complex problems which arise in very different sectors, such as image processing, design of control and diagnostic systems [32, 33]. The problem to be solved can often be considered as an optimization problem in

✉ Boumediene Selma, selma.boumediene@yahoo.fr; Samira Chouraqui, s_chouraqui@yahoo.fr; Hassane Abouaïssa, hassane.abouaissa@univ-artois.fr | [1]Département d'Informatique, Université des Sciences et de la Technologie d'Oran USTO'MB, 31000 Oran, Algérie. [2]Laboratoire de Génie Informatique et d'Automatique de l'Artois (LGI2A), Univ. Artois, EA 3926, 62400 Bethune, France.

which one or more objective functions, are defined that one seeks to minimize or maximize by contributing to all the parameters concerned. The resolution of such a problem has led researchers to propose more and more efficient methods of resolution, among which we can cite metaheuristics [34–41].

In the artificial intelligence practice, the controller parameters are chosen from among knowledge bases extracted by learning algorithms [42–45]. By using such practices, the obtained parameters are too far to be optimal [46–48]. Therefore, mathematical optimization techniques have received much attention as methods to obtain optimized parameters.

Recently a lot of work based on the optimization of controllers can be found in the literature, such as authors in [49], proposed a fuzzy controller using a bee colony algorithm (BCO) used in order to optimize benchmark control problems. In [50] a type-2 fuzzy logic controller is optimized with the traditional BCO. In [51], ACO algorithm was implemented as tuning mechanism for proportional integral (PI) controller, applied to a SMAR® didactic level plant. An ACO is used to easy search for the optimal PI controller parameters, proposed for a speed control of switched reluctance motor supplied by photovoltaic system in [52]. Using ACO to optimize proportional–integral–derivative (PID) controller parameters, for wind turbine tower disturbances has been studied in [53]. In [54] an ACO is employed to determine the optimal PI controller parameters for speed control to get high performance of maximum power point tracking. A fully tuned RBF neural network controller based on ACO algorithm and Lyapunov functions has been used for ultrasound hyperthermia cancer tumor therapy in [55]. In [56] authors presented the optimal trajectory tracking control of robotic manipulator using an ACO algorithm based PID controller. An optimal design of PID using particle swarm optimization algorithm (PSO) for the control of five bar linkage robot has been introduced in [57]. A PSO algorithm for fuzzy predictive control has been developed and applied for quadruple-tank process in [58]. Authors in [59] have improved a PID controller method by ACO optimization in order to find the optimal parameters for the stabilization control of quadrotor. In [60], a gradient decent optimization is used to tune PID parameters for a quadrotor UAV. An optimization technique to adjust the LQR and PID controller parameters applied to control inverted pendulum was presented in [61].

Intelligent tools as neural networks and fuzzy logic are now increasingly used in the modeling, design and control law of complex systems. They attract attention, and have become the most important controllers of the last decades, and they have been implemented on different nonlinear dynamic systems, to solve the input saturation, dead-zone, and unmodeled dynamics [62–65].

In this paper, a robust non-linear controller for trajectory tracking tasks accomplished by a three degree of freedom quadrotor nonlinear closed-loop. An adaptive neuro-fuzzy (ANFIS) controller is implemented to a multivariable nonlinear quadrotor to accurately reproduce a desired trajectory in 2D vertical plane.

This paper is organized as follows. The description of the UAV model and the problem formulation are given in Sect. 2. ANFIS system with its architecture and learning algorithm are introduced in Sect. 3. The conventional ACO algorithm is presented in Sect. 4. The purpose of Sect. 5 is to present the IACO algorithm that will later be used for the optimization of ANFIS parameters. Section 6 details the proposed control design and strategy. In Sect. 7, comparisons and numerical simulations results are given in order to demonstrate the optimal effectiveness of the proposed controller. Section 8 gives the conclusions.

2 Model description and problem formulation

2.1 Description of the quadrotor model

It is primordial to introduce the reference coordinates in which we describe the full structure, before describing the mathematical model of the quadrotor. The quadrotor body is with y, z axes. As shown in Fig. 1, the origin located in the center of the quadrotor. It is known that the quadrotor with a three degree of freedom (3 DOF). The Euler angle ϕ represent the orientation, where it is roll angle about the horizontal axis.

So the quadrotor is modeled to fly in 2 dimensions *yz* plane with an angle ϕ witch is the roll angle as shown in Fig. 1.

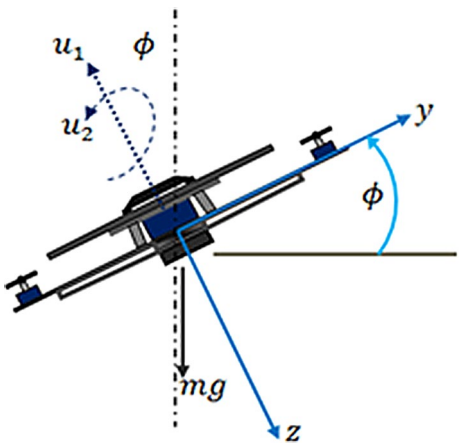

Fig. 1 Quadrotor configuration design

The state of the quadrotor is therefore $[y, z, \phi]^T$ and there are two inputs u_1 and u_2, which represent the thrust and the moment about the x-axis respectively.

2.2 Equation of motion

Since our drone is modeled in two dimensions, we have y and z plane and a roll angle ϕ as seen before. The equations describing the movement are written as follows:

$$\ddot{y} = \frac{u_1}{m}\sin(\phi). \tag{1}$$

$$\ddot{z} = g - \frac{u_1}{m}\cos(\phi). \tag{2}$$

$$\ddot{\phi} = \frac{u_2}{I_{xx}}. \tag{3}$$

where m and I_{xx} are the mass and the moment of inertia, respectively.

The equations of motion have been rewriting in the form below,

$$\begin{bmatrix} \ddot{y} \\ \ddot{z} \\ \ddot{\varphi} \end{bmatrix} = \begin{bmatrix} 0 \\ g \\ 0 \end{bmatrix} + \begin{bmatrix} \frac{1}{m}sin\phi & 0 \\ -\frac{1}{m}cos\phi & 0 \\ 0 & \frac{1}{I_{zz}} \end{bmatrix} \begin{bmatrix} u_1 \\ u_2 \end{bmatrix}. \tag{4}$$

The state space description of the quadrotor,

$$\mathrm{x} = \begin{bmatrix} \mathrm{x}_1 \\ \mathrm{x}_2 \end{bmatrix} = \begin{bmatrix} y \\ z \\ \varphi \\ \dot{\mathrm{y}} \\ \dot{z} \\ \dot{\varphi} \end{bmatrix}. \tag{5}$$

So, the first derivative of the state vector is presented in Eq. (6). The first three parameters of the vector represent velocities and the last three parameters represent accelerations.

$$\dot{x} = \begin{bmatrix} \dot{y} \\ \dot{z} \\ \dot{\varphi} \\ 0 \\ g \\ 0 \end{bmatrix} + \begin{bmatrix} 0 & 0 \\ 0 & 0 \\ 0 & 0 \\ \frac{1}{m}sin\phi & 0 \\ -\frac{1}{m}cos\phi & 0 \\ 0 & \frac{1}{I_{zz}} \end{bmatrix} \begin{bmatrix} u_1 \\ u_2 \end{bmatrix}. \tag{6}$$

The vector $[u_1, u_2]$ is the input signals that can drive the dynamical system, by specifying the properties of u_1 and u_2 we can change the state of the quadrotor.

Looking at motion equations we know it's a non-linear system, the nonlinearity here comes only from the fact that we have $\cos(\phi)$ and $\sin(\phi)$ for both $\ddot{y}$ and $\ddot{z}$ equations [Eqs. (1), (2)].

Since system is not linear, we need to perform a linearization, let's consider that the motion equations have a hover configuration.

2.3 Equilibrium hover configuration

Only when the thrust vector u_1 and the gravity vector are opposed, the hover configuration will be in equilibrium. The system is linearized near the hover point, where the properties are:

$$y_0, z_0, \phi_0 = 0, u_{1,0} = mg, u_{2,0} = 0,$$

2.4 Linearized dynamics model

We know that the $sin(\phi)$ and $cos(\phi)$ are the two sources of the non-linearity, so when ϕ is close to zero $sin(\phi)$ behave basically like ϕ and $cos(\phi)$ becomes nearly constant.

$$\mathrm{y} = \mathrm{mgm} \cdot \ddot{\mathrm{s}}\mathrm{in}\Delta\phi \rightarrow \mathrm{g}\phi. \tag{7}$$

$$\ddot{z} = g - \frac{u_1}{m} \cdot cos\Delta\phi \rightarrow g - \frac{u_1}{m}. \tag{8}$$

$$\ddot{\phi} = \frac{u_2}{I_{xx}}. \tag{9}$$

If we replace $sin(\phi)$ by ϕ and $cos(\phi)$ by 1 we get the linear equations see below,

$$\ddot{y} = g\phi. \tag{10}$$

$$\ddot{z} = g - \frac{u_1}{m}. \tag{11}$$

$$\ddot{\phi} = \frac{u_2}{I_{xx}}. \tag{12}$$

3 ANFIS system

The proposed neuro-fuzzy network is a five-layer architecture that includes the elements of a fuzzy Sugeno-type system [66–68] (Fig. 2). Looking at Fig. 3, let's explain how the network works layer-by-layer.

Layer 1 (Fuzzification): This layer contains adaptive nodes. The outputs are the fuzzy membership grade of the inputs, which are given by:

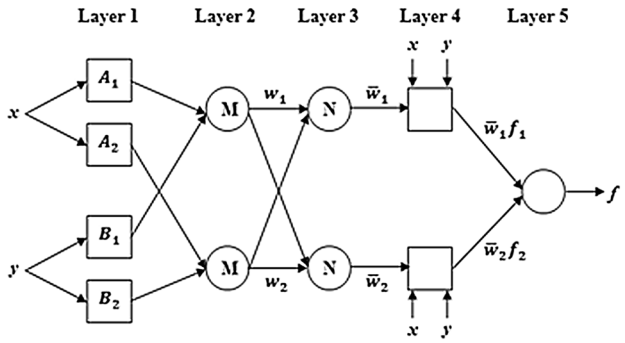

Fig. 2 The equivalent typical ANFIS architecture

$$O_i^1 = \mu_{A_i}(x), \quad i = 1,2. \tag{13}$$

$$O_j^1 = \mu_{B_j}(y), \quad j = 1,2. \tag{14}$$

where μ_{A_i}, μ_{B_j} denote the membership degrees obtained from this layer.

Fuzzifying the inputs is conducted by MF such as Piecewise linear, triangular, trapezoidal, Gaussian and Singleton. Among the abovementioned MFs, this paper has used the Gaussian function because of its smooth and concise notation. Therefore as $\mu_{A_i}(x)$, given that.

$$\text{Triangular}: \mu_{A_i}(x) = max\left(min\left(\frac{x-a_i}{b_i-a_i}, \frac{c_i-x}{c_i-b_i}\right), 0\right), \quad i = 1,2. \tag{15}$$

$$\text{Trapezoidal}: \mu_{A_i}(x) = max\left(min\left(\frac{x-a_i}{b_i-a_i}, 1, \frac{d_i-x}{d_i-c_i}\right), 0\right), \quad i = 1,2. \tag{16}$$

$$\text{Gaussian}: \mu_{A_i}(x) = exp\left(-\frac{(x-c_i)^2}{{\sigma_i}^2}\right), \quad i = 1,2. \tag{17}$$

where a_i, b_i, c_i and σ_i are the premise parameters.

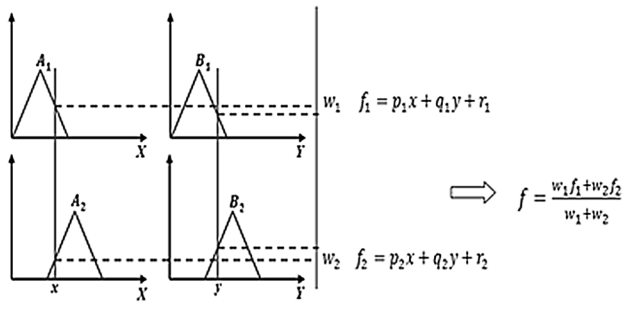

Fig. 3 A 2 inputs first order Sugeno type model with 2 rules

Layer 2 (Weighting of fuzzy rules): The symbol M shows every fixed node in this layer. This layer calculates the firing strength w_k by using membership values computed in fuzzification layer, and the outputs are computed as the following:

$$O_k^2 = w_k = \mu_{A_i}(x) * \mu_{B_j}(y), \quad i,j = 1,2. \tag{18}$$

Layer 3 (Normalization): Every node is fixed node and called by N. Each node obtains the normalization by calculating the ratio of the kth rule's firing strength (truth values) to the sum of all rules firing strength. The output O_k^3 at this step is given by:

$$O_k^3 = \bar{w_k} = \frac{w_k}{\sum w_i} = \frac{w_k}{w_1 + w_2}, \quad k = 1,2. \tag{19}$$

Layer 4 (Defuzzification): weighted consequent values of rules are calculated in each node of this layer as given in Eq. (21).

$$O_k^4 = \bar{w_k} f_k = \bar{w_k}\left(p_k x + q_k y + r_k\right), \quad k = 1,2. \tag{20}$$

where w_k represents the output of the third layer, and $\{p_k, q_k, r_k\}$ are consequent.

Layer 5 (Summation): The actual output is obtained by summing the outputs of all incoming signals that coming from the defuzzification layer to produce the overall ANFIS output.

$$O^5 = \sum_{k=1}^{2} \bar{w_k} f_k = \frac{\sum_{1=1}^{2} w_k * f_k}{w_1 + w_2}. \tag{21}$$

4 Ant colony optimization algorithm

ACO is a biomimetic optimization technique inspired by the work of a biologist [69] taken up by computer scientists [70], and exploited and developed by Marco Dorigo in the 1990s [71], 1991 [72]. The idea is to mimic the behavior of the real ants that collaborate, for example for the search for food sources by mixing random exploration behavior and monitoring the chemical traces left by their sisters. These chemical traces, the "pheromones", are used by ants to communicate indirectly, through the environment, a general technique known to entomologists as stigmergy. It is this form of communication as well as the idea of cooperating a host of simple and localized agents that forms the basis of the heuristics developed by Dorigo.

First applied to the travelling sales person (TSP) problem as a multi-agent solution, colony optimization of ants has quickly proved its effectiveness in the context of combinatorial optimization in general and has been

particularly beneficial for the problem of routing information packets in large interconnection networks. Ant colony optimization now forms, with its twin sister particle swarm optimization [73], a field of research in its own right, swarm intelligence [74], or even, as its scope goes beyond combinatorial problems to tackle multi-purpose problems or design problems cognitive and parameters tuning as is the case in this study, a new manner to design agents-based artificial intelligence.

The fundamental idea of ACO algorithm is based on the behavior of natural ant colonies, that of a parallel search through numerous computational threads based on a problem data and on a dynamic memory structure. This memory contains informations on the quality of the different solutions previously obtained to the optimization problem under consideration. The communication of the different search agents is a collective behavior that has proved to be highly effective in solving combinatorial optimization problems.

Ants will work in parallel to try different solutions to a given problem until they find a better one. We proceed as follows:

At the start of each iteration, the ants are randomly placed on the nodes. Each ant starts its "tour": it moves from node to another node without ever visiting one that it has already seen and until it has visited all the nodes of the graph. The choice of the transition from a node i to a node j is randomly based on a probability given by the Eq. (22).

$$P_{ij}^{k}(t) = \frac{\left(\left[\tau_{ij}(t)\right]^{\alpha}\left[\eta_{ij}\right]^{\beta}\right)}{\sum_{i\in N_i}\left[\tau_{ij}(t)\right]^{\alpha}\left[\eta_{ij}\right]^{\beta}}. \tag{22}$$

$\tau_{ij}(t)$: The amount of pheromones on the edge (i,j).
η_{ij}: Visibility value between edge (i,j) or heuristic information value, and also called it the desirability of edge (i,j).
α: Constant factor that control the influence of τ_{ij}. If $\alpha = 0$, the probability of selecting the closer nodes is higher. In fact, in this condition ACO is converted to a stochastic search algorithm.
β: Constant factor that control the influence of η_{ij}. If $\beta = 0$, only the pheromone information is utilized. In this case, there will be a faster convergence of the algorithm.
N_i: Set of the node points that haven't visited yet.

Ants will move from any node i to another node j with this probability. Once all ants have complete their tours or iterations, after all the nodes are visited. Amount of pheromone is updated by increasing the pheromone levels, according to the Eq. (23) [69].

$$\tau_{ij}(t+1) = (1-\rho)\tau_{ij}(t) + \Delta\tau_{ij}(t). \tag{23}$$

ρ: Coefficient of pheromone evaporation $(0 < \rho < 1)$.
$\Delta\tau_{ij}(t)$: The amount of pheromone on edge (i,j). This amount is calculated by Eq. (24).

$$\Delta\tau_{ij}(t) = \sum_{k=1}^{m}\Delta\tau_{ij}^{k}. \tag{24}$$

m: Total number of ants.
$\Delta\tau_{ij}^{k}$: The quantity of pheromone deposited by ant k on edge (i,j).

Equation (25) shows the contribute amount of the (k) ant to the pheromone trace at the any edge (i,j) [74].

$$\Delta\tau_{ij}^{k} = \frac{Q}{L_k}. \tag{25}$$

Q: A constant, often equal to 1.
L_k: The tour length (cost) of the kth ant.
If the ant used the edge (i,j) along the tour, trace amount is calculated according to Eq. (25). Otherwise, the trace amount is zero [74].

The fact that the pheromone evaporates over time is extremely important because it allows the ant colony to rely on constantly updated information. In an artificial ants system, it is important to implement a form of evaporation to avoid the system remaining "stuck" in a local optimum and to open the door to the expected characteristics of dynamic adaptivity.

The ACO metaheuristic algorithm is shown in Fig. 4.

The advantage of using the ACO over other optimization methods;

(1) Search among a population in parallel.
(2) Give a rapid discovery of good solutions.
(3) Adapt to changes, such as new distances.
(4) Have guaranteed convergence.
(5) Used in dynamic applications.

5 Improved ant colony optimization

5.1 Ant path selection

IACO is a probabilistic method designed to solve complex problems as ACO. The optimal combination problems

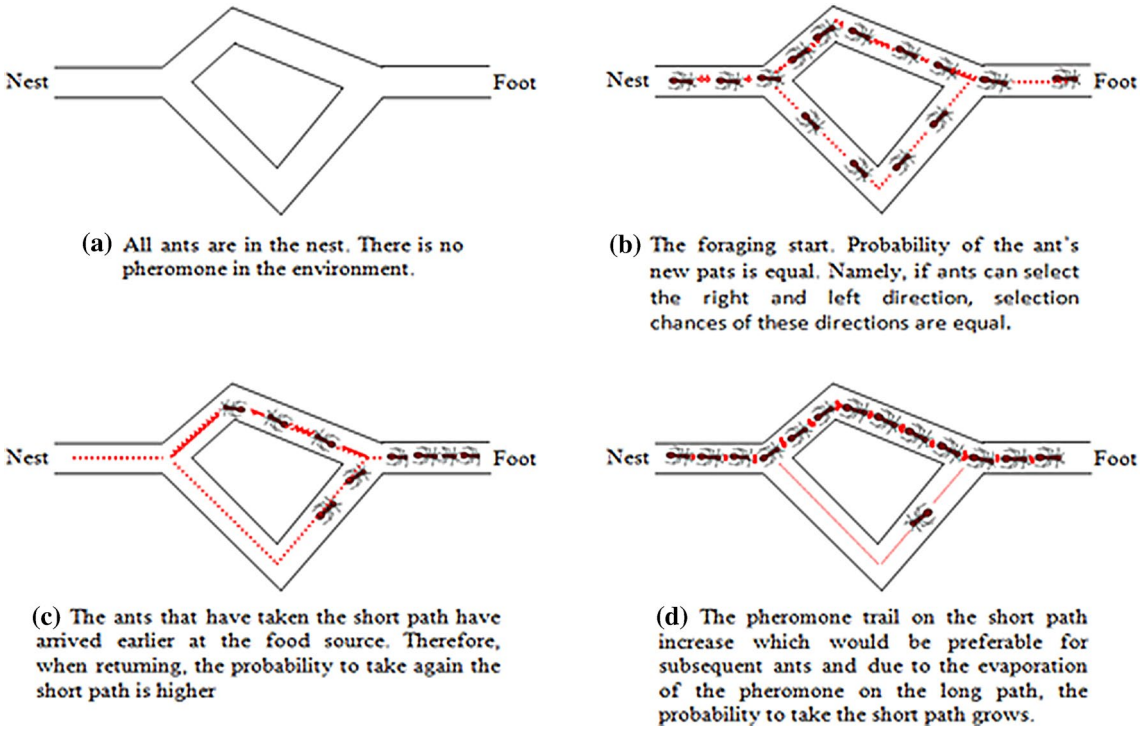

Fig. 4 An experimental demonstration which proves the captivity of the ants to find the shortest way leading to a food source

which can be solved by IACO can be represented by a graph $G(N, E)$, where, N denotes the nodes, and E denotes the edges linking with the nodes. The difficulties of IACO are the construction of ant colony search paths and values of corresponding parameters.

Ants carry a certain amount of pheromone, during the process of visit the next nodes, ants will release the pheromone on the path between the visited nodes. Pheromones will evaporate over time, therefore, the shorter paths will have more pheromones, and more pheromones and more ants will attracted to select in the next iteration. The probability that ants choose the next node to be visited is

$$P_{ij}^{k}(t) = \begin{cases} \dfrac{\left([\tau_{ij}(t)]^{\alpha}[\eta_{ij}]^{\beta}\right)}{\sum_{i\in N_i}[\tau_{ij}(t)]^{\alpha}[\eta_{ij}]^{\beta}}, & j \in J_k \\ 0, & otherwise \end{cases} \tag{26}$$

Where J_k is the set of unvisited states of the kth ant in the ith population.

In the ACO algorithm, the pheromone updating is a key problem, it includes the local pheromone updating and the global pheromone updating. In order to improve the optimization performance of the ACO algorithm in solving complex optimization problem, the new strategy to update the increased pheromone and pheromone diffusion mechanism are proposed to improve the ACO algorithm.

5.2 The local pheromone updating strategy

Before the first iteration of the ACO algorithm is executed, the pheromones on each edge are equal constants. When any ant in the ACO algorithm completes the current iteration, the strategy to update local pheromone is carried out on the each passed edge for ant. The expression of the local pheromone updating strategy is described as follow:

$$\tau_{ij}(t+1) = (1-\rho_L)\tau_{ij}(t) + \rho_L \Delta\tau_{ij}(t). \tag{27}$$

$$\Delta\tau_{ij}(t) = \sum_{k=1}^{m} \Delta\tau_{ij}^{k} \tag{28}$$

$$\Delta\tau_{ij}^{k}(t) = \begin{cases} \frac{Q}{L_K}, & ant\ k\ go\ through\ edge\ (i,j), \\ 0, & otherwise \end{cases} \tag{29}$$

Where, ρ_L $(0 < \rho_L < 1)$, is local pheromone evaporating coefficient, $1 - \rho_L$ is the pheromone residue factor.

Here, Q is the total number of pheromone taken by ant, L_K denotes the total length of the paths gone through by ant k in this iteration.

5.3 The global pheromone updating strategy

In one iteration, after all ants in the ACO algorithm complete their solutions, the passed nodes are carried out the

global pheromone updating strategy. The expressions of the local pheromone updating strategy are described as follows:

$$\tau_{ij}(t+1) = (1-\rho_G)\tau_{ij}(t) + \rho_G \Delta\tau_{ij}(t). \tag{30}$$

$$\Delta\tau_{ij}(t) = \sum_{k=1}^{m} \Delta\tau_{ij}^{k} \tag{31}$$

$$\Delta\tau_{ij}^{k} = \begin{cases} \frac{1}{L_s}, (i,j) \in \text{the optimal paths}, \\ 0, otherwise \end{cases} \tag{32}$$

Where, ρ_G ($0 < \rho_G < 1$), is global pheromone evaporating coefficient, $1-\rho_G$ is the pheromone residue factor, L_S is the total length of the current optimal paths.

The ways of ending the algorithm as follows:

(a) Setting the maximum number of iteration;
(b) Setting the error of the system;
(c) The optimal paths not change, that is to say, the algorithm is convergent.

The advantages of IACO as follows:

(1) IACO inherits the inherent advantages of ACO, such as strong robustness, multiple objective coordination, positive and negative feedback, parallelism and fast convergence speed.
(2) Global update of the pheromone trail is helpful to increase the probability that ants choose the current optimal paths, and thus, attracts more ants transfer to the current optimal paths. By this way, it will reduce the search scope to improve the efficiency;
(3) The strategy of updating the global pheromone trails is easy, and not complex as the elite ant colony system, which is based on ranking. Therefore, performing the global pheromone trails update has not affect on improving the whole efficiency of the algorithm.

6 Controller design

An adaptive controller represented by an automatically tuning ANFIS by an IACO algorithm for a better and optimal choice of those parameters whose parameter adaptation law is responsible for reducing the tracking errors and which is due to the simplified dynamics.

The auto-tuning (self-optimization) of ANFIS parameters is specifically to find the optimal design of the membership functions (MFs) in the neuro-fuzzy controller by an ant colony algorithm leads to automatically adjusting the fuzzy rules because the two parts (membership functions and fuzzy rules) cannot be dissociated. Moreover, the optimization by the IACO, whose sole objective is the improvement of a numerical criterion, often leads to the presence of more precise fuzzy rules at the end of the optimization process which leads to better results. It is within this framework that our motives and interests lie in the design of neuro-fuzzy controllers by ant colony algorithms.

In our study an ANFIS controller applied to a totally autonomous UAV tracking trajectory, modeled to fly in 2 dimensions (yz) plane with an angle ϕ which is the roll angle, both y and z equations that describe the trajectory and the roll angle ϕ are considered as an objective function. To improve controller, an optimization method based on the evolutionary algorithms. IACO is proposed to obtain the optimal parameters leading to the optimal or ideal trajectory and therefore to completion of the specified movement resets the control.

The trajectory to follow is defined by the vector R_T, which consisting of two elements $\{y(t), z(t)\}$ as shown in Fig. 5.

Given the reference trajectory

$$R_T(t) = \begin{bmatrix} y(t) \\ z(t) \end{bmatrix}. \tag{33}$$

And the measured trajectory is defined by the vector R_C

$$R_C(t) = \begin{bmatrix} y_C(t) \\ z_C(t) \end{bmatrix}. \tag{34}$$

where $y_C(t)$ and $z_C(t)$ are the calculated parameters by the controller.

For each parameter defining the trajectory, we consider a controller with two inputs, the error $e(t)$ and its variation $\Delta e(t)$ and an output $\Delta u(t)$, the variation of the command, which allows to adjust to each moment the command $u(t)$, applied to the system (Fig. 6). The fuzzy rules constituting the base of the controller, in this case, have two premises.

The proposed controller uses to represent the objective function which is allows optimal control of the intelligent UAV and an IACO algorithm to obtain the optimal

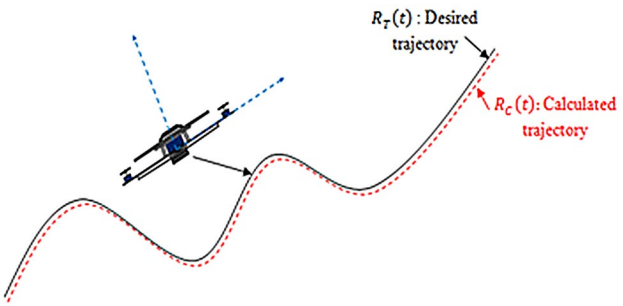

Fig. 5 Quadrotor trajectory tracking in 2D plane

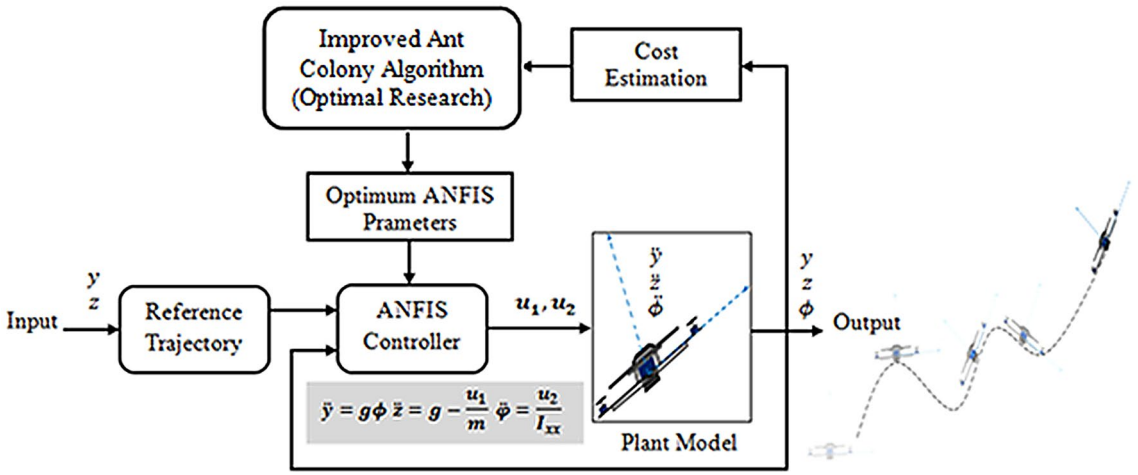

Fig. 6 Optimization of ANFIS controller with IACO block diagram

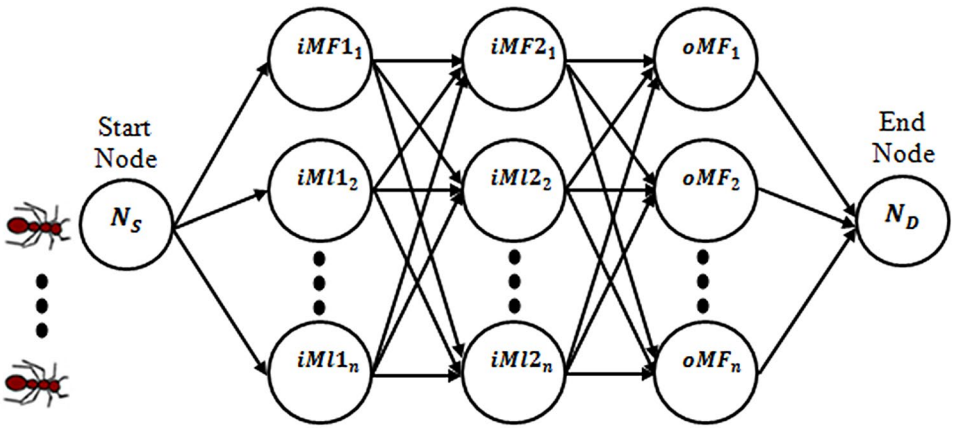

Fig. 7 IACO for ANFIS tuning process

objective value. The optimization process of the ANFIS controller by ACO block schema is given in Fig. 7.

To optimize the parameters of the ANFIS controller by improved ACO, we first need to create the controller design. This hybridization can be represented as a graph, which is given in Fig. 7. All the values of the parameters $(iMF1_i, iMF2_i, oMF_i)$ can be considered as three vectors and each parameter contains three parameters that define the membership functions as shown above, which $iMF1_i$, $iMF2_i$ and oMF_i are the MFs of the first input, the second input and the output respectively. In order to create a representation in graph form correspond to the problem, these three vectors represent paths between the start node and the end node. To make a complete tour, each ant must visit the three nests by following path between start node and end node. IACO's objective is to find the optimal tour that has the lowest cost function.

In a neuro-fuzzy controller, each linguistic variable is defined by a set of membership functions of the language terms, and fuzzy rules are applied to linguistic terms. These terms, which qualify a linguistic variable, are defined through MFs.

The membership function is defined by parameters like the triangular one as shown in Fig. 3, it is defined by three parameters x_1, x_2 and x_3 which take their values in the interval $[a, b]$. The Fig. 3 illustrates an example of fuzzy partitioning with 2 triangular MFs.

The optimization procedure consists in finding the best adjustment of the parameters of the MFs of each control variable.

In general, the objective of a control system is to minimize the difference $e(t)$ between the output of a system and a desired output. This difference may be due either to a setpoint change or to disturbances acting on the system. This objective can be defined by several numerical indices. Only the desired behavior can be a paramount parameter to take into account to make a good choice among these indices. In our remarks, we have opted for the minimization of the mean squared error (MSE) and root mean squared error (RMSE).

After selecting the IACO parameters, an equal number of pheromones were given to the roads that all artificial ants can use and this value was kept at the pheromone matrix. When the first artificial ant leaves the nest, it chooses a random path because there is an equal amount of pheromone on accessible roads and completes the tour by visiting three nests. At the end of the tour, the simulation was performed and executed with selected ANFIS parameters, and the value of the roads passing by the artificial ants at pheromone matrix was updated by calculating the RMS error between the reference path input and output of the simulation, which is the cost function. To ensure that the following artificial ants do not go the same way on the road, the pheromone table has also been updated by multiplying a random number. Thus, the ants tried to track the given reference trajectory by different ANFIS parameters in each tour. When some artificial ants complete the tour, the pheromone amount at the path of the artificial ant that has the least RMS error in this tour is increased and the pheromone amount at the path of the artificial ant that has a maximum RMS error in this tour is reduced than the amount of the good ant. In addition, the pheromone amount at the roads taken by all artificial ants are evaporated with an evaporation constant (ρ). If the RMS error is low with selected ANFIS parameters, the next ants try to complete their work of winding these parameters. When the maximum lap is completed, the routes with a maximum value at the pheromone table, that is, the selected ANFIS parameters, are recorded as a result of the optimization. When the maximum tour is completed, the roads that have a maximum value at the pheromone table, that is, the selected ANFIS parameters, are recorded as a result of the optimization.

The evolution of the cost function of the IACO is reduced after each iteration until it reaches the optimal controller ANFIS parameters.

7 Simulation results

In order to control an UAV moving along a specified trajectory. The model was implemented in Matlab/Simulink programming software, a simulation was made for illustrative purpose. The UAV is commanded to flight following a pre-defined trajectory as a function of time defined by $y(t)$ and $z(t)$.

The proposed approach involves two main steps. First, the experimental data are ready to train and test the ANFIS system to represent the objective function. Finally, an improved ACO algorithm is used to obtain the optimal objective value. In this study, all MFs have been chosen to be Gaussian-shaped. During the learning of ANFIS, the experimental data sets were used to perform 100 training cycles.

We build an ants population from the starting set and we try to perform an exploration to find good subsets and retain those that have a good accuracy rate. It is a procedure for setting ANFIS parameters in an automatic way.

The control performance obtained by the proposed control system is compared with those obtained by, PID and ANFIS controllers to validate the superior performance of the studied controller.

The simulation results are obtained with a vertical trajectory in 2D space. The desired trajectory input is defined as:

$y_d(t) = 2sin(t)$ and $z_d(t) = 5sin(t)$

The parameters of the quadrotor used in the following simulations are shown in Table 1.

Table 1 Parameters of quadrotor

Symbol	Value
m	0.2 kg
I_{xx}	0.1 kg m^2
g	9.81 m/s^2

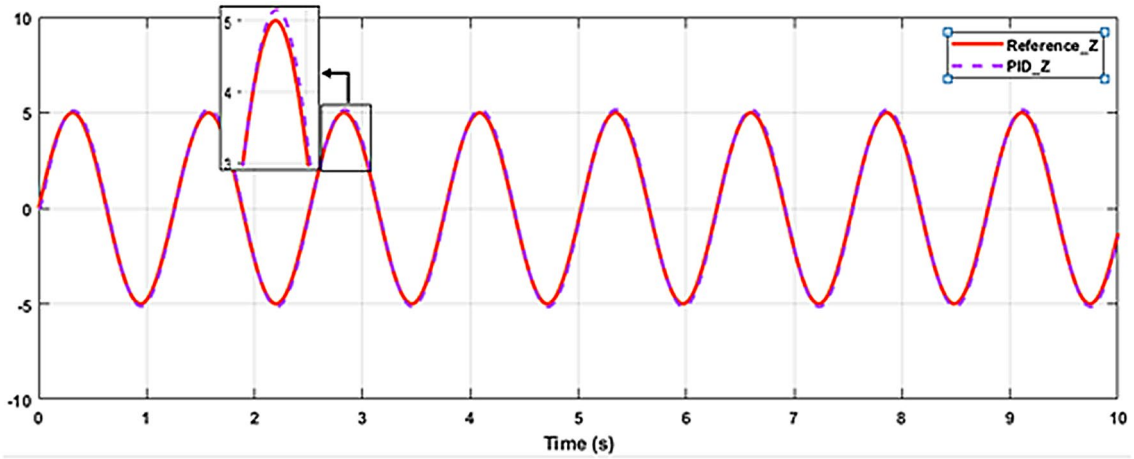

Fig. 8 PID *z* measured

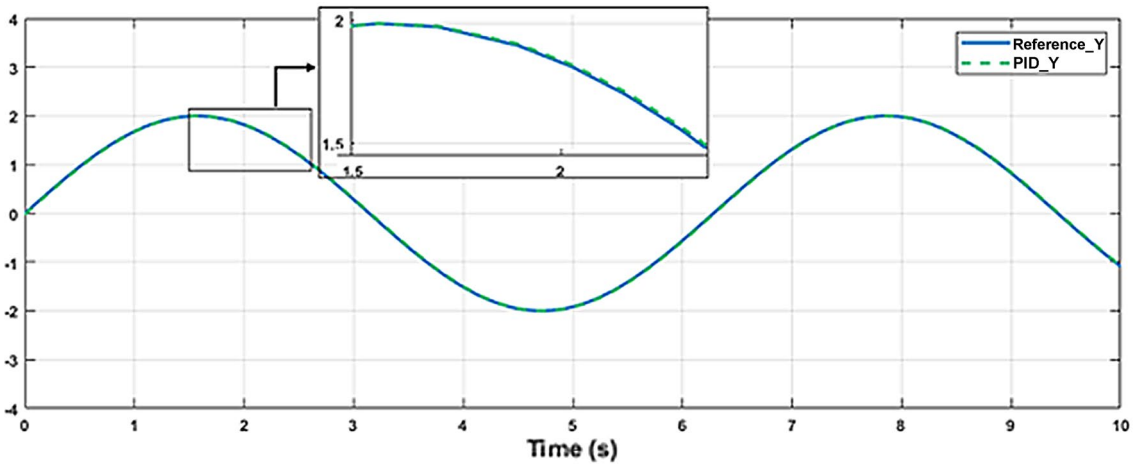

Fig. 9 PID *y* measured

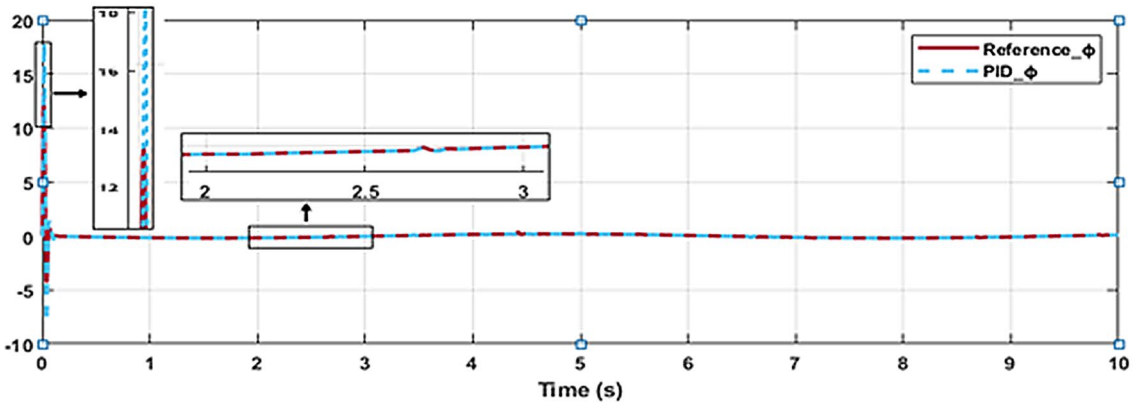

Fig. 10 PID ϕ measured

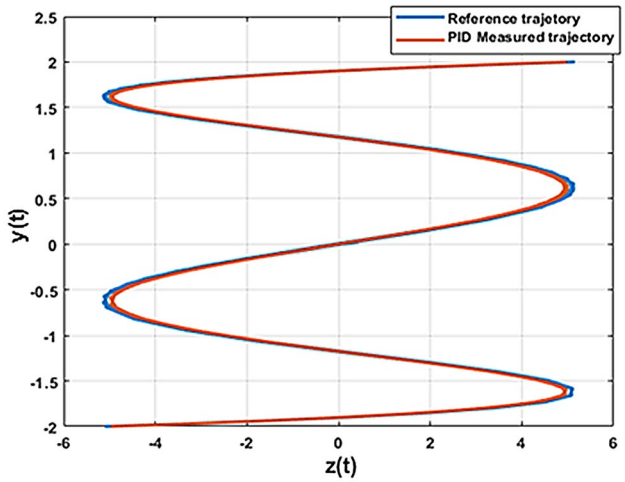

Fig. 11 PID trajectory measured

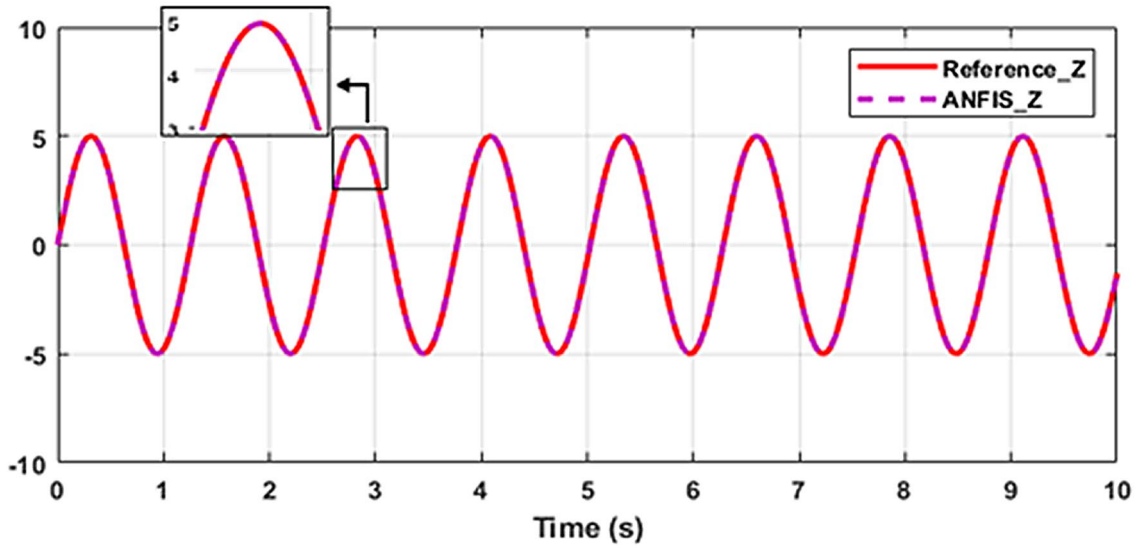

Fig. 12 ANFIS *z* measured

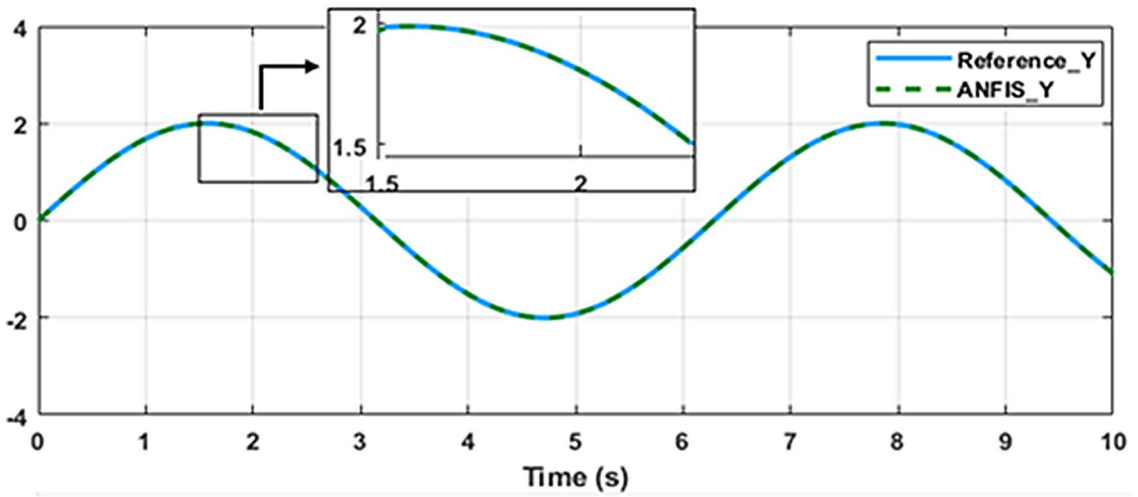

Fig. 13 ANFIS *y* measured

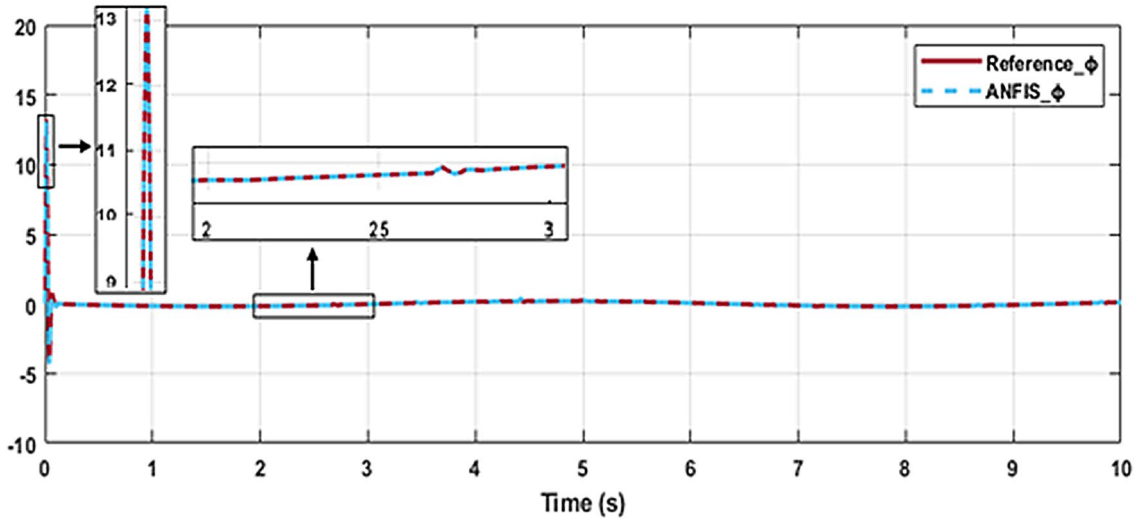

Fig. 14 ANFIS ϕ measured

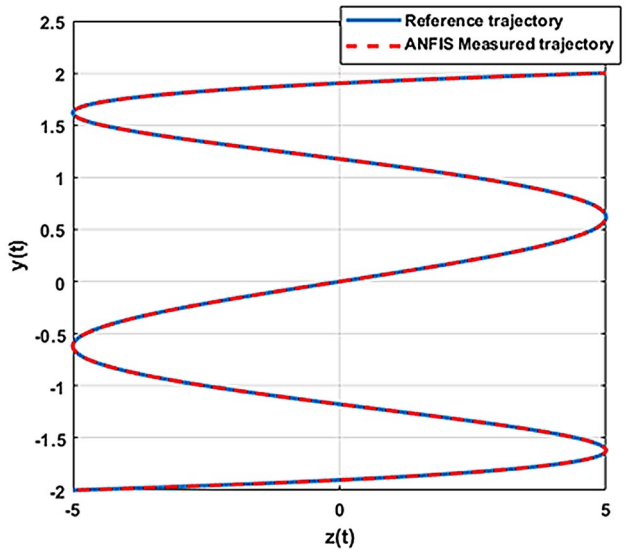

Fig. 15 ANFIS trajectory measured

Finally, the three control inputs y, z, ϕ were shown below.

Trajectory tracking simulation has been presented in this section, and some simulation results are given to illustrate the control performances of the developed controller. The trajectory tracking responses of the three used controllers are shown in Figs. 11, 15 and 25 from which it can be observed that the desired reference trajectory can be tracked effectively by the proposed ANFIS-IACO controller.

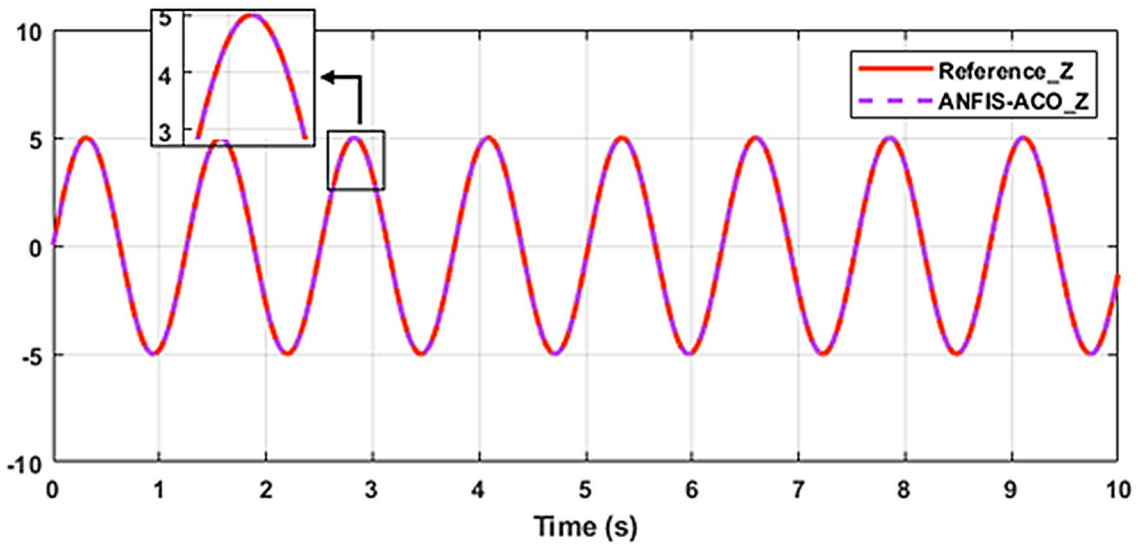

Fig. 16 ANFIS-IACO z measured

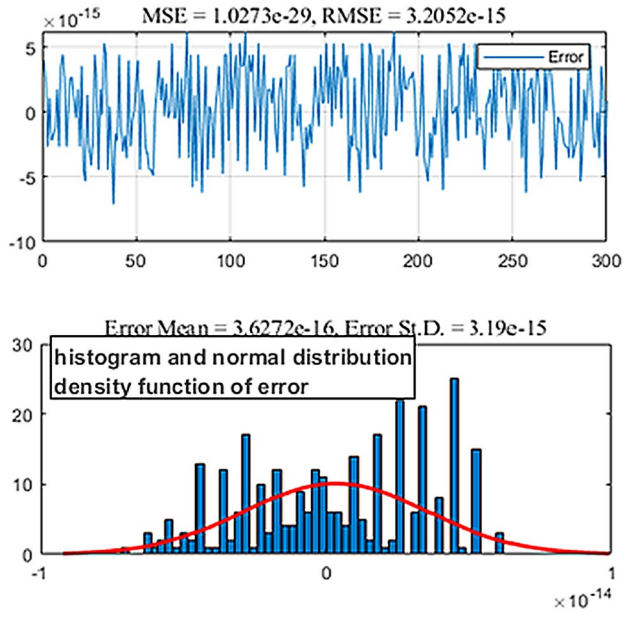

Fig. 17 Error test data (*z* parameter)

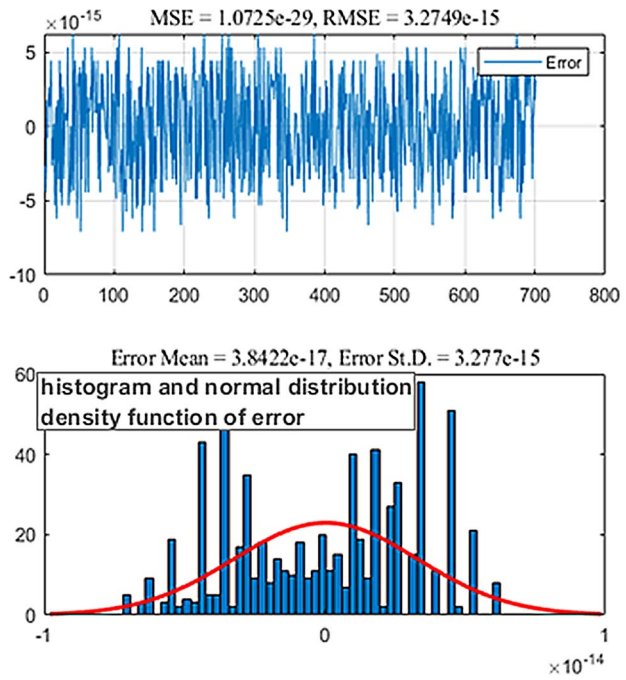

Fig. 18 Error train data (*z* parameter)

With the evaluation of the results, it's seen that ANFIS-IACO controller has successfully followed the reference but PID controller has given the poor results compared to other controllers.

Figures 8, 9, 10 and 11 showed the PID results, this controller can reproduce the tracking trajectory with error of MSE $= 6.42 \times 10^{-2}$ and RMSE $= 0.25$.

The simulation result obtained by the neuro-fuzzy system is given in Figs. 12, 13, 14 and 15. It can be seen that realizes a good approximation of the system with an error MSE $= 5.47 \times 10^{-10}$ and RMSE $= 2.34 \times 10^{-5}$.

Figures 16, 17 and 18 showed the ANFIS-IACO simulation results. The tracking performance is illustrated in Fig. 25, where the measured trajectory of the UAV and the reference trajectory are shown together. The results obtained show that the performances of our hybrid approach are superior to those of the other models. The validity of the proposed model was proved by mean square error MSE $< 10^{-29}$ and MSE $< 10^{-14}$. Figures 19, 20, 21, 22, 23 and 24 shows the trajectory tracking parameters errors of the proposed controller. It can be clearly seen that the trajectory tracking errors is zero.

The improved ACO algorithm provides an improvement, by comparing ANFIS performances with the same ANFIS optimized by improved ACO, a significant increase in accuracy. A clear improvement of the precision in the trajectory tracking is thus visible. The RMSE used to measure the accuracy of the control model, decreases by 10^9 times (Fig. 25).

We used an evolutionary algorithm approach that is ACO. An improved ACO exploration of this search space is performed to identify subsets of more relevant parameters, and accurate by a new membership function distribution, that adapts well to each linguistic variable, that leads to minimizing the error between the desired trajectory and the calculated one.

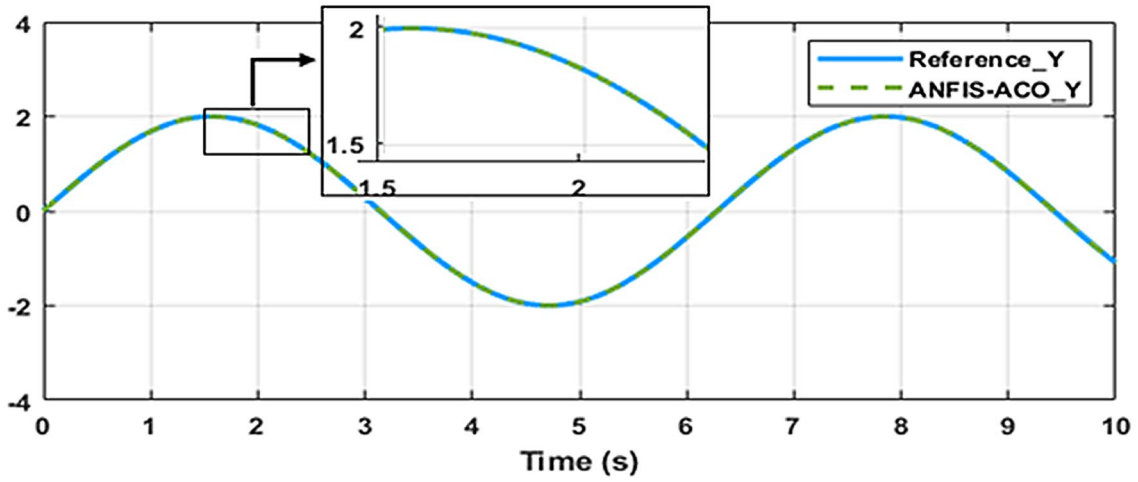

Fig. 19 ANFIS-IACO *y* measured

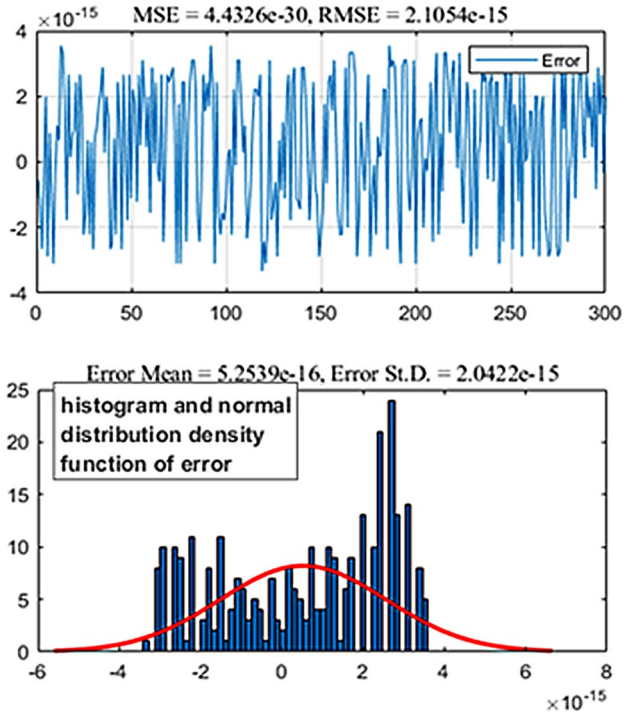

Fig. 20 Error test data (*y* parameter)

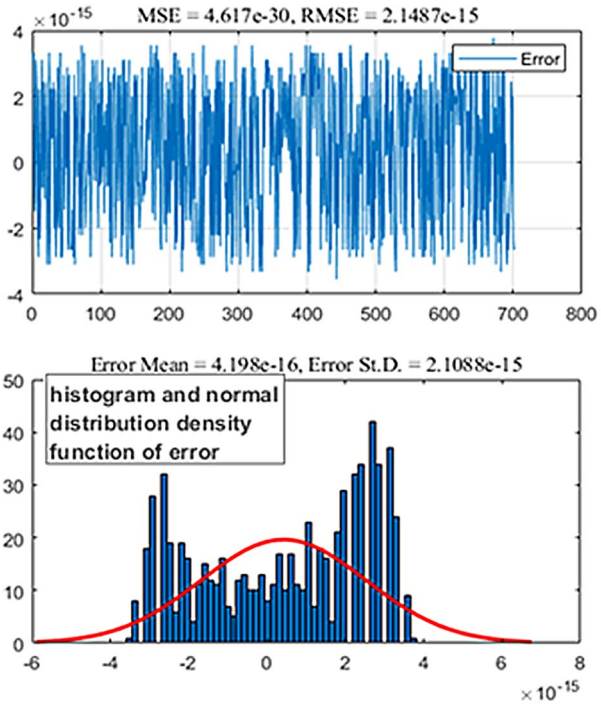

Fig. 21 Error train data (*y* parameter)

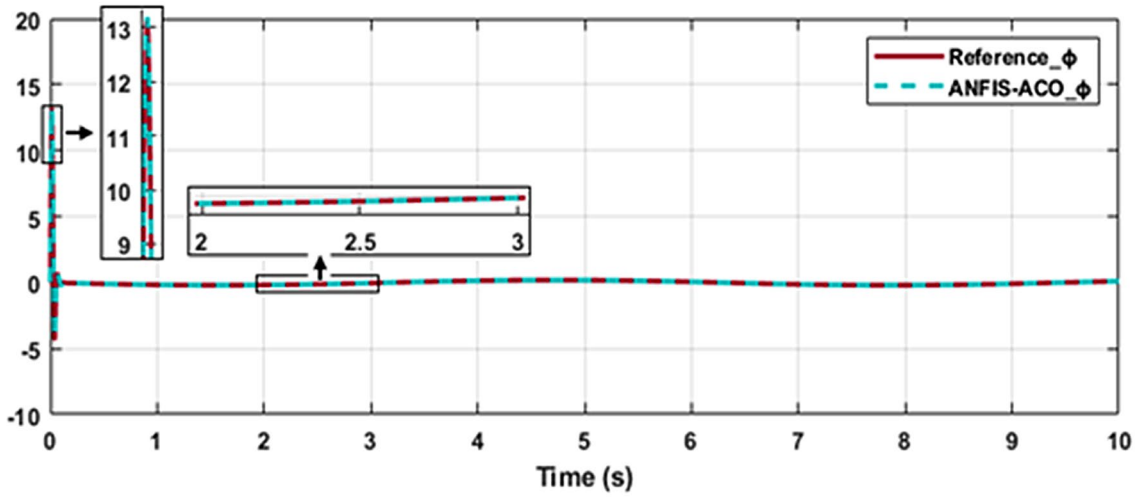

Fig.22 ANFIS-IACO ϕ measured

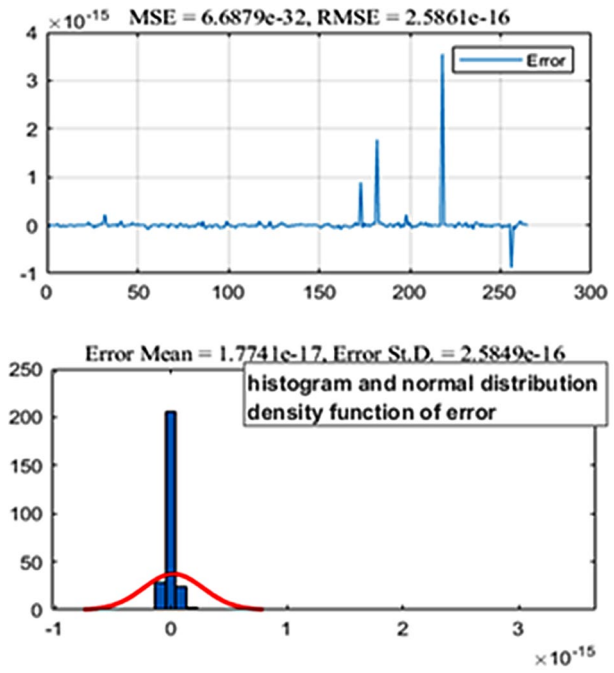

Fig. 23 Error test data (ϕ parameter)

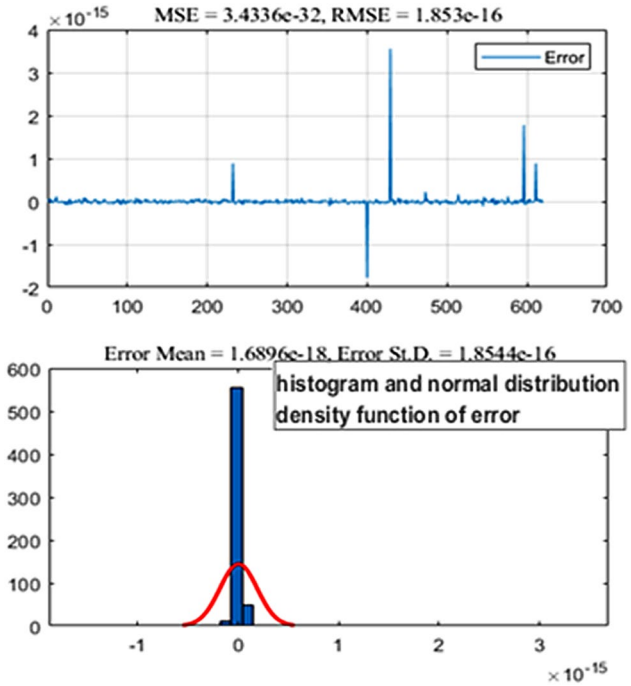

Fig. 24 Error train data (ϕ parameter)

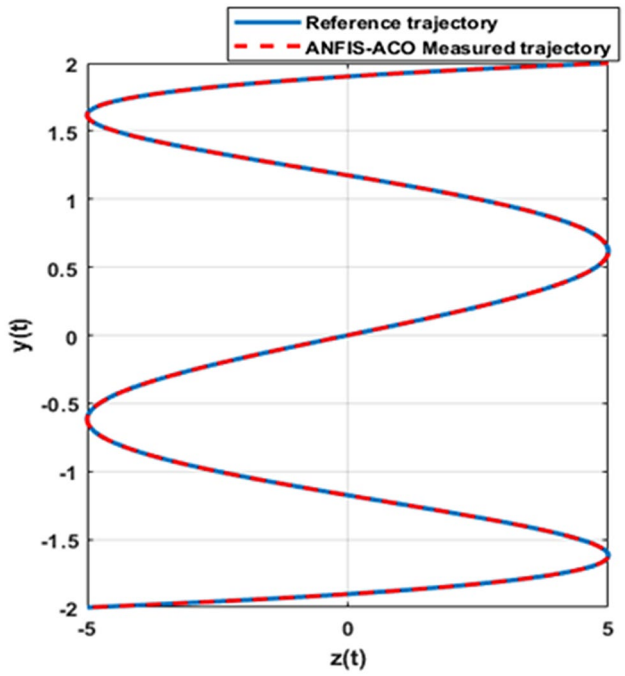

Fig. 25 ANFIS-IACO measured trajectory

8 Conclusion

The tracking performance using tuned fuzzy neural network parameters with ant colony optimization (ANFIS-IACO) algorithm of a quadrotor unmanned vehicle is investigated in this study.

The computer simulation results depict that the proposed optimized fuzzy ANFIS-IACO controller performance outperforms the PID and ANFIS controllers. Several reference signals were tested to evaluate the tracking performance where the outcomes demonstrate that the proposed ANFIS-IACO controller was able to minimize the error and bring the quadrotor to the desired trajectory and reached to a steady state in short time period. In addition, RMSE error was reduced significantly using the proposed controller.

Through this study which was based on the development and the application of artificial intelligence techniques in nonlinear systems control, it is showed that:

- Neuro-fuzzy networks like ANFIS present a powerful tool in the control of non-linear systems.
- The evolutionary algorithm IACO is dedicated to the optimization of the ANFIS parameters and represents a precise intelligent solution.
- The correct choice of the parameters of the ANFIS algorithm, IACO is subject to the robustness of the laws based on last.

Compliance with ethical standards

Conflict of interest The authors declare that they have no conflict of interest.

Ethical approval This article does not contain any studies with human participants or animals performed by any of the authors.

Informed consent Informed consent was obtained from all individual participants included in the study.

References

1. Mostafa SA, Ahmad MS, Mustapha A (2019) Adjustable autonomy: a systematic literature review. Artif Intell Rev 51:149–186
2. Mahadevan P (2010) The military utility of drones, no 78. CSS Analysis in Security Policy. Center for Security Studies (CSS), ETH Zurich
3. Bujak A, Smolarek M, Gebczynska A (2011) Applying military telematic solutions for logistics purposes. In: 11th international conference on transport systems telematics, pp 248–256
4. Haidari LA, Brown ST, Ferguson M, Bancroft E, Spiker M, Wilcox A, Ambikapathi R, Sampath V, Connor DL, Lee BY (2016) The economic and 432 operational value of using drones to transport vaccines. Vaccine 34:4062–4067. https://doi.org/10.1016/j.vaccine.2016.06.022
5. Barmpounakis EN, Vlahogianni EI, Golias JC (2016) Unmanned aerial systems for transportation engineering: current practice and future challenges. Int J Transp Sci Technol 5:111–122
6. Reinartz P, Lachaise M, Schmeer E, Krauss T, Runge H (2006) Traffic monitoring with serial images from airborne cameras. ISPRS J Photogramm Remote Sens 61:149–158. https://doi.org/10.1016/j.isprsjprs.2006.09.009
7. European Aviation Safety Agency (2016) "Prototype" commission regulation on unmanned aircraft operations. https://www.easa.europa.eu/sites/default/files/dfu/UAS%20Prototype%20Regulation%20final.pdf
8. Siebert S, Teizer J (2014) Mobile 3D mapping for surveying earthwork projects using an unmanned aerial vehicle (UAV) system. Autom Constr 41:1–14. https://doi.org/10.1016/j.autcon.2014.01.004
9. Valente J, Cerro JD, Barrientos A, Sanz D (2013) Aerial coverage optimization in precision agriculture management: a musical harmony inspired approach. Comput Electron Agric 99:153–159
10. Freeman PK, Freeland RS (2014) Politics & technology: U.S. polices restricting unmanned aerial systems in agriculture. Food Policy 49:302–311. https://doi.org/10.1016/j.foodpol.2014.09.008
11. Lenhart D, Hinz S, Leitloff J, Stilla U (2008) Automatic traffic monitoring based on aerial image sequences. Pattern Recognit Image Anal 18:400–405. https://doi.org/10.1134/S1054661808030061
12. Puri A, Valavanis K, Kontitsis M (2007) Statistical profile generation for traffic monitoring using real-time UAV based video data. Mediterr Conf Control Autom. https://doi.org/10.1109/MED.2007.4433658
13. Kanistras K, Martins G, Rutherford MJ, Valavanis KP (2014) Survey of unmanned aerial vehicles (UAVs) for traffic monitoring. In: Valavanis KP, Vachtsevanos GJ (eds) Handbook of unmanned aerial vehicles. Springer, Cham, pp 2643–2666. https://doi.org/10.1109/ICUAS.2013.6564694

14. Chow JYJ (2016) Dynamic UAV-based traffic monitoring under uncertainty as a stochastic arc-inventory routing policy. Int J Transp Sci Technol 5(3):167–185
15. Srinivasan S, Latchman H, Shea J (2004) Airborne traffic surveillance systems: video surveillance of highway traffic. In: Proceedings of ACM 2nd international workshop on video surveillance sensor networks, pp 131–135
16. Farradyne P (2005) Use of unmanned aerial vehicles in traffic surveillance and traffic management. Technical Memorandum for Florida Department of Transportation
17. Finn RL, Wright D (2012) Unmanned aircraft systems: surveillance, ethics and privacy in civil applications. Comput Law Secur Rev 28:184–194. https://doi.org/10.1016/j.clsr.2012.01.005
18. Ma L, Li MC, Wang YF, Tong LH, Cheng L (2013) Using high-resolution imagery acquired with an autonomous unmanned aerial vehicle for urban construction and planning. In: Proceedings of 2013 international conference on remote sensing, environmental and transportation engineering (Rsete 2013), vol 31, pp 200–203
19. Dobson RJ, Brooks C, Roussi,C, Colling T (2013) Developing an unpaved road assessment system for practical deployment with high-resolution optical data collection using a helicopter UAV. In: International conference on unmanned aircraft systems (ICUAS), IEEE, pp 235–243. https://doi.org/10.1109/ICUAS.2013.6564695
20. Knyaz VA, Chibunichev AG (2016) Photogrammetric techniques for road surface analysis. In: ISPRS-international archives of the photogrammetry, remote sensing and spatial information sciences, Prague, Czech Republic, pp 515–520. https://doi.org/10.5194/isprsarchives-XLI-B5-515-2016
21. Hoffer NV, Coopmans C, Jensen AM, Chen Y (2014) A survey and categorization of small low-cost unmanned aerial vehicle system identification. J Intell Robot Syst 74:129–145
22. Kanellakis C, Nikolakopoulos G (2017) Survey on computer vision for UAVs: current developments and trends. J Intell Robot Syst 87:141–168
23. Watts AC, Ambrosia VG, Hinkley EA (2012) Unmanned aircraft systems in remote sensing and scientific research: classification and considerations of use. Remote Sens 4:1671–1692
24. Di Franco C, Buttazzo G (2016) Coverage Path Planning for UAVs Photogrammetry with Energy and Resolution Constraints. J Intell Robot Syst 83:445–462
25. Artemenko O, Dominic OJ, Andryeyev O, Mitschele-Thiel A (2016) Energy-aware trajectory planning for the localization of mobile devices using an unmanned aerial vehicle. In: Proceedings of the 2016 25th international conference on computer communication and networks (ICCCN), Waikoloa, HI, USA, 1–4 August 2016, pp 1–9
26. Cabreira TM, Di Franco C, Ferreira PR Jr, Buttazzo GC (2018) Energy-aware spiral coverage path planning for UAV photogrammetric applications. IEEE Robot Autom Lett 3:3662–3668
27. Vincent P, Rubin I (2004) A framework and analysis for cooperative search using UAV swarms. In: Proceedings of the a framework and analysis for cooperative search using UAV swarms, Nicosia, Cyprus, 14–17 March 2004, pp 79–86
28. Xu A, Viriyasuthee C, Rekleitis I (2011) Optimal complete terrain coverage using an unmanned aerial vehicle. In: Proceedings of the 2011 IEEE international conference on robotics and automation, Shanghai, China, 9–13 May 2011, pp 2513–2519
29. Xu A, Viriyasuthee C, Rekleitis I (2014) Efficient complete coverage of a known arbitrary environment with applications to aerial operations. Auton Robots 36:365–381
30. Chen H, Xu J (2015) Exploring optimal controller parameters for complex industrial systems. In: IEEE international conference on cyber technology in automation, control, and intelligent systems (CYBER), Shenyang, 2015, pp 383–388. https://doi.org/10.1109/CYBER.2015.7287967
31. Hekimoğlu B (2019) Optimal tuning of fractional order PID controller for DC motor speed control via chaotic atom search optimization algorithm. IEEE Access 7:38100–38114. https://doi.org/10.1109/ACCESS.2019.2905961
32. Chrouta J, Chakchouk W, Zaafouri A, Jemli M (2019) Modeling and control of an irrigation station process using heterogeneous cuckoo search algorithm and fuzzy logic controller. IEEE Trans Ind Appl 55(1):976–990. https://doi.org/10.1109/TIA.2018.2871392
33. Al-Dhaifallah M, Nassef AM, Rezk H, Nisar KS (2018) Optimal parameter design of fractional order control based INC-MPPT for PV system. Sol Energy 159:650–664
34. Sekhar GTC, Sahu RK, Baliarsingh AK, Panda S (2016) Load frequency control of power system under deregulated environment using optimal firefly algorithm. Int J Electr Power Energy Syst 74:195–211
35. Ranjania M, Murugesan P (2015) Optimal fuzzy controller parameters using PSO for speed control of quasi-Z source DC/DC converter fed drive. Appl Soft Comput 27:332–356
36. Hasanien HM (2018) Performance improvement of photovoltaic power systems using an optimal control strategy based on whale optimization algorithm. Electr Power Syst Res 157:168–176
37. Rahman M, Ong ZC, Chong WT et al (2019) Wind turbine tower modeling and vibration control under different types of loads using ant colony optimized PID controller. Arab J Sci Eng 44(2):707–720. https://doi.org/10.1007/s13369-018-3190-6
38. Rajesh KS, Dash SS, Rajagopal R (2018) Hybrid improved firefly-pattern search optimized fuzzy aided PID controller for automatic generation control of power systems with multi-type generations. Swarm Evol Comput. https://doi.org/10.1016/j.swevo.2018.03.005
39. Zhou Y, Miao F, Luo Q (2019) Symbiotic organisms search algorithm for optimal evolutionary controller tuning of fractional fuzzy controllers. Appl Soft Comput 77(497–508):1568–4946. https://doi.org/10.1016/j.asoc.2019.02.002
40. Bounar N, Labdai S, Boulkroune A (2019) PSO–GSA based fuzzy sliding mode controller for DFIG-based wind turbine. ISA Trans 85(177–188):0019–0578. https://doi.org/10.1016/j.isatra.2018.10.020
41. Bai L, Feng YW, Li N, Xue XF (2019) Optimal fuzzy iterative learning control based on artificial bee colony for vibration control of piezoelectric smart structures. J Vibroeng 21(1):111–132. https://doi.org/10.21595/jve.2018.19698
42. Varsek A, Urbancic T, Filipic B (1993) Genetic algorithms in controller design and tuning. IEEE Trans Syst Man Cybern 23(5):1330–1339. https://doi.org/10.1109/21.260663
43. Mendes J, Araújo R, Matias T, Seco R, Belchior C (2014) Automatic extraction of the fuzzy control system by a hierarchical genetic algorithm. Eng Appl Artif Intell 29:70–78. https://doi.org/10.1016/j.engappai.2013.12.012
44. Vasičkaninová A, Bakošová M (2015) Control of a heat exchanger using neural network predictive controller combined with auxiliary fuzzy controller. Appl Therm Eng 89:1046–1053
45. Soliman MA, Hasanien HM, Azazi HZ, El-kholy EE, Mahmoud SA (2018) Hybrid ANFIS-GA-based control scheme for performance enhancement of a grid-connected wind generator. IET Renew Power Gener 12(7):832–843. https://doi.org/10.1049/iet-rpg.2017.0576
46. Ram SS et al (2016) Designing and comparison of controllers based on optimization techniques for pH neutralization process. In: 2016 international conference on information communication and embedded systems (ICICES)

47. Ribeiro JMS, Santos MF, Carmo MJ, Silva MF (2017) Comparison of PID controller tuning methods: analytical/classical techniques versus optimization algorithms. In: 2017 18th international Carpathian control conference (ICCC), pp 533–538 https://doi.org/10.1109/CarpathianCC.2017.7970458
48. Hafez AT, Givigi SN, Yousefi S (2018) Unmanned aerial vehicles formation using learning based model predictive control. Asian J Control 20:1014–1026. https://doi.org/10.1002/asjc.1774
49. Caraveo C, Valdez F, Castillo O (2012) Optimization of fuzzy controller design using a new bee colony algorithm with fuzzy dynamic parameter adaptation. Appl Soft Comput 43:131–142
50. Castillo O, Amador-Angulo L (2018) A generalized type-2 fuzzy logic approach for dynamic parameter adaptation in bee colony optimization applied to fuzzy controller design. Inf Sci 460:476–496
51. Gonçalves LC, Santos MF, de Sa RJF, da Silva JL, Rezende HB et al (2018) Development of a PI controller through an ant colony optimization algorithm applied to a SMAR® didactic level plant. In: 19th international Carpathian control conference (ICCC), IEEE
52. Oshaba AS, Ali ES, Abd Elazim SM (2017) Speed control of SRM supplied by photovoltaic system via ant colony optimization algorithm. Neural Comput Appl 28:365. https://doi.org/10.1007/s00521-015-2068-8
53. Rahman M, Ong ZC, Chong WT et al (2019) Wind turbine tower modeling and vibration control under different types of loads using ant colony optimized PID controller. Arab J Sci Eng 44:707. https://doi.org/10.1007/s13369-018-3190-6
54. Mokhtari Y, Rekioua D (2018) High performance of maximum power point tracking using ant colony algorithm in wind turbine. Renew Energy 126:1055–1063
55. Karar ME, El-Brawany MA (2018) Fully tuned RBF neural network controller for ultrasound hyperthermia cancer tumour therapy. Netw Comput Neural Syst. https://doi.org/10.1080/0954898X.2018.1539260
56. Singh R, Prasad LB (2018) Optimal trajectory tracking of robotic manipulator using ant colony optimization. In: 5th IEEE Uttar Pradesh section international conference on electrical, electronics and computer engineering (UPCON), Gorakhpur, India, 2018, pp 1–6. https://doi.org/10.1109/UPCON.2018.8597087
57. Aghababa MP (2016) Optimal design of fractional-order PID controller for five bar linkage robot using a new particle swarm optimization algorithm. Soft Comput 20:4055. https://doi.org/10.1007/s00500-015-1741-2
58. Thamallah A, Sakly A, M'Sahli F (2019) A new constrained PSO for fuzzy predictive control of quadruple-tank process. Meas J Int Meas Confed 136:93–104
59. Priyambodo TK, Putra AE, Dharmawan A (2015) Optimizing control based on ant colony logic for quadrotor stabilization. In: IEEE international conference on aerospace electronics and remote sensing technology (ICARES), Bali, 2015, pp 1–4. https://doi.org/10.1109/ICARES.2015.7429820
60. Babu VM, Das K, Kumar S (2017) Designing of self tuning PID controller for AR drone quadrotor. In: 18th international conference on advanced robotics (ICAR), Hong Kong, 2017, pp 167–172. https://doi.org/10.1109/ICAR.2017.8023513
61. Jacknoon A, Abido MA (2017) Ant colony based LQR and PID tuned parameters for controlling inverted pendulum. In: International conference on communication, control, computing and electronics engineering (ICCCCEE), Khartoum, 2017, pp 1–8. https://doi.org/10.1109/ICCCCEE.2017.7867652
62. Van M (2019) Adaptive neural integral sliding-mode control for tracking control of fully actuated uncertain surface vessels. Int J Robust Nonlinear Control 29:1537–1557. https://doi.org/10.1002/rnc.4455
63. Zhang S, Dong Y, Ouyang Y, Yin Z, Peng K (2018) Adaptive neural control for robotic manipulators with output constraints and uncertainties. IEEE Trans Neural Netw Learn Syst. https://doi.org/10.1109/TNNLS.2018.2803827
64. Yang T, Sun N, Chen H, Fang Y (2019) Neural network-based adaptive antis-wing control of an under-actuated ship-mounted crane with roll motions and input dead-zones. IEEE Trans Neural Netw Learn Syst. https://doi.org/10.1109/TNNLS.2019.2910580
65. Sun N, Yang T, Fang Y, Wu Y, Chen H (2018) Transportation control of double-pendulum cranes with a nonlinear quasi-PID scheme: design and experiments. IEEE Trans Syst Man Cybern Syst. https://doi.org/10.1109/TSMC.2018.2871627
66. Jang JSR (1993) ANFIS: adaptive-network-based fuzzy inference systems. IEEE Trans Syst Man Cybern 23(3):665–685
67. Walia N, Singh H, Sharma A (2015) ANFIS: adaptive neuro-fuzzy inference system—a survey. Int J Comput Appl 123:32–38
68. Karaboga D, Kaya E (2018) Adaptive network based fuzzy inference system (ANFIS) training approaches: a comprehensive survey. Intell Rev Artif. https://doi.org/10.1007/s10462-017-9610-2
69. Manderick B, Moyson F (1988) The collective behaviour of ants: an example of self-organisation in massive parallelism. Technical report: AI-memo 1988-7
70. Deneubourg JL, Pasteels JM, Verhaeghe JC (1983) Probabilistic behaviour in ants: a strategy of errors? J Theor Biol 105:259–271
71. Colorni A, Dorigo M, Maniezzo V (1991) Distributed optimization by ant colonies. In: Proceedings of the first European conference on artificial life, MIT Press/Bradford Book, Paris
72. Dorigo M (1992) Optimization, learning and natural algorithms. PhD thesis, Dipartimento di Electronica, Politecnico di Milano, IT
73. Kennedy J, Eberhart RC (2001) Swarm intelligence. Morgan Kaufmann Publishers, San Francisco
74. Bonabeau E, Dorigo M, Theraulaz G (1999) Swarm intelligence: from natural to artificial systems. Oxford University Press, Oxford. ISBN 0-19-513159-2